



# Simulation of thermal stress within diffusion couple of composite seals with Crofer 22APU for solid oxide fuel cells applications



Gurbinder Kaur<sup>a,\*</sup>, D. Homa<sup>a</sup>, K. Singh<sup>b</sup>, O.P. Pandey<sup>b</sup>, B. Scott<sup>a</sup>, G. Pickrell<sup>a</sup>

<sup>a</sup> Department of Material Science and Engineering, Virginia Tech, Holden Hall, Blacksburg, VA 24060, USA

<sup>b</sup> School of Physics and Materials Science, Thapar University, Patiala 147004, India

## HIGHLIGHTS

- Sealing and bonding issues of composite glass sealants made by ball milling have been analyzed.
- Thermal stress has been simulated for glass composite/Crofer 22APU diffusion couple.
- COMSOL multiphysics has been used to simulate studies for 10,000 h of operation of SOFC.
- The heat-flux is also simulated to understand any temperature gradient.

## ARTICLE INFO

### Article history:

Received 12 May 2013

Received in revised form

19 May 2013

Accepted 20 May 2013

Available online 29 May 2013

### Keywords:

Glass composite

Solid oxide fuel cell (SOFC)

COMSOL

Simulation

Thermal stress

Solidworks

## ABSTRACT

The appropriate selection of component material is a critical issue for technological development of SOFC. Hence, the main aim of this paper is to investigate the sealing and bonding issues in solid oxide fuel cells (SOFC) using COMSOL multiphysics analysis. Using multiphysics modeling, the stress generated within the composite seal after 10,000 h heat-treatment at 800 °C along with its magnitude was simulated. The thermal stress was also investigated as a function of seal thickness. Interestingly, for all the diffusion couples, no high stress regions were observed at the corners. For most of the GG5 surface, the stress varies between 0.4 and 0.8 N m<sup>-2</sup> for seal thickness of 0.5 mm, which is the highest among all samples having same thickness. The heat-flux was simulated in order to investigate if there was any temperature gradient about the interface, or within the layers. Isothermal contours were obtained for the sample GG7 upto 1000 °C for 10,000 h heat-treatment.

© 2013 Elsevier B.V. All rights reserved.

## 1. Introduction

Due to increased concerns about environment by the impact of harmful gas emissions, there is need of clean and efficient power sources. Hence, planar solid oxide fuel cells (pSOFC) are attracting much attention due to their wide range of applications and eco-friendly nature [1–5]. Moreover, the energy obtained in pSOFC is through electrolytic reactions unlike fossil fuels, further enhancing its efficiency. pSOFC require hermetic seals in order to avoid leakage losses as well as maintenance of separation between fuel and oxidant [6–9]. Hence, it is important to design the seals in a way that satisfies the criteria of electric insulation, chemical compatibility and matching coefficient of thermal expansion with adjacent components [10–12].

Composite seals have been potential candidates for sealing as their flexure strength as well as fracture toughness is higher than glass seals [13]. In previous work, researchers in this group used a new novel approach of making composite glass seals by mixing them in fixed ratio and then ball milling for 5 h, which could address the chromate formation, coefficient of thermal expansion CTE, and sealing capability along with improved viscosity without dispersing any filler material (unreactive) in glass matrix [14]. Chemically, the composite of two glassy materials is more compatible to each other further reducing the thermal stress at working temperature of SOFCs. Seals are exposed to reducing/oxidizing atmospheres at an average temperature between 800 and 1000 °C for an anticipated duration of 10,000–20,000 h. At such temperatures, crystallization may occur leading to change in thermal, mechanical and chemical properties of composite seals [15–17]. These changes affect the mechanical integrity as well as compatibility of seal with adjoining components leading to residual

\* Corresponding author. Tel.: +1 540 239 7929.

E-mail address: [gkaur82@vt.edu](mailto:gkaur82@vt.edu) (G. Kaur).

thermal stresses within stack [18]. Hence, it is very important to address the thermal stress generated in the cell stack for uninterrupted working of SOFC.

The stress generated within the diffusion couple of Crofer 22APU and composite seals made from glasses by ball milling have not been explored. In our previous work, novel glass-composite seals were developed to address the sealing capability, chromate formation and improved viscosity along with CTE without dispersing filler material (unreactive) in glass matrix. The idea behind this approach is to avoid the stress within sealing materials due to segregation of filler particles at high temperatures. At the same time, the composite of two glassy materials is chemically more compatible to each other, which can further reduce the thermal stress at working temperature of SOFCs. Moreover, high-energy ball milling helps in obtaining a uniform and homogenized glass composite with improved particle size, viscosity and adhesion behavior. Keeping all these points in consideration and in continuation to our previous work on composites [14], this paper describes the thermal stress generated within glass-composite seals/Crofer 22APU assembly. In addition to this, the effect of seal thickness on the thermal stress has also been investigated. These studies were carried out using COMSOL multiphysics analysis. Using multiphysics analysis, the stress generated within modeled composite seals after 10,000 h heat-treatment at 800 °C along with its magnitude was simulated. It is necessary to predict these stresses due to the CTE mismatch because the thermal properties of the seal material must be superior as it is difficult to repair any failure in seal during cell-operation.

## 2. Modeling parameters

The 30AO–20B<sub>2</sub>O<sub>3</sub>–40SiO<sub>2</sub>–10La<sub>2</sub>O<sub>3</sub> (A = Mg, Ca, Sr, Ba) glasses have been prepared using melt-quenching techniques and labeled as ML, CL, SL and BL respectively. The preparation details are given elsewhere [10,11]. These glass compositions are mixed in ratio 1:1 and then ball-milled for 5 h [14]. The composition with sample labels is shown in Table 1. COMSOL multiphysics 4.3.0.151 software is used to carry out three-dimensional stress analysis of diffusion couples i.e. glass composite/Crofer 22APU. The model is constructed using solidworks standard 2009 and the file is imported as a 3D CAD file. The fine mesh was configured within both components as shown in Fig. 1(a). A “mesh” is mapped on all surfaces of the model, which defines thousands of small areas, called elements, for which stresses, strains and temperatures are calculated. Hence, the software is able to evaluate physical effects with an adjustable resolution. For constructing the mesh, three degrees of freedom were chosen. The accuracy of model is highly dependent on the nature of mesh and it increases as the mesh size becomes extra fine. At the same time, if the mesh becomes finer, the computational time increases. Hence, the mesh size is selected to optimize both the accuracy and the computational time. The Crofer 22APU alloy has a thickness of 2 mm and the composite thickness (*t*) is 0.25, 0.5 and 1.5 mm respectively. In our previous investigations [14], the thickness of composite seal was taken to be 0.5 mm for

investigation on interfacial interaction with Crofer 22APU. The thickness of 1.5 mm for the glass composite has been chosen in order to investigate the stress distribution, when the composite thickness is comparable to the thickness of Crofer 22APU. The composition, CTE and density used for composite materials to analyze COMSOL studies are listed in Table 1. Two user-defined models are used i.e. thermal stress and heat transfer. The models are time dependent as the stress generated can be obtained after very step with a relative tolerance of ±0.01. To study the thermal stress for prolonged heat-treatment duration of 10,000 h, the program was scheduled from 0 to 3.6E7 s with a step size of 1. The convergent solutions are obtained for all the diffusion couples. The convergent solution of the non-linear solver and time dependent solver (BDF) for GG1/Crofer 22APU are shown in Fig. 1(b) and (c) respectively. The solid model is taken to be isotropic with global coordinate system. The temperature range is chosen to be room temperature (RT) – 800 °C. The heat-flux model was also studied in order to understand the temperature difference in layers after the 10,000 h treatment.

## 3. Results and discussion

Whenever structures made from two different materials are subjected to a temperature change, they can experience thermo-mechanical stress attributed to differences in the material properties and temperature gradient. Basically, the seal failure occurs due to two reasons. First is the interfacial delamination near the joint region [19] and second is the crack within the seal [20,21]. If the interfacial fracture energy is lower than the fracture energy of seal, then the failure at the interface may occur or vice-versa.

In the present study, both the components have been assembled as a layered system. Layered materials are usually subjected to thermal residual stress, hence making them more prone to cracking [22]. The CTE mismatch between the seal and adjoining components can cause compressive thermal stress ( $CTE_{\text{glass}} > CTE_{\text{comp}}$ ) or tensile thermal stress ( $CTE_{\text{comp}} > CTE_{\text{glass}}$ ) at the interface [4]. These stresses are formed due to the dislocations, particularly, at the boundary of the two components. Ultimately, the presence of these dislocations leads to formation of cracks and pores (tensile stress) delamination of glass seal (compressive/shear stress). All the glass composites possess lower CTE than the metallic interconnect ( $11.3 \times 10^{-6} \text{ K}^{-1}$ ), which can make them undergo a biaxial compressive stress  $\sigma$ . But at the free surfaces of the composite seal, tensile stress may dominate. The 3D stress can be expressed in tensor form as follows:

$$\sigma = \begin{pmatrix} \sigma_{xx} & \sigma_{xy} & \sigma_{xz} \\ \sigma_{yx} & \sigma_{yy} & \sigma_{yz} \\ \sigma_{zx} & \sigma_{zy} & \sigma_{zz} \end{pmatrix} \quad (1)$$

But recently, more general form of the Von-Mises stress is given as follows [23]:

$$\sigma = \left( \frac{1}{\sqrt{2}} \right) \left[ (\sigma_x - \sigma_y)^2 + (\sigma_y - \sigma_z)^2 + (\sigma_z - \sigma_x)^2 + 6(I_{xy}^2 + I_{yz}^2 + I_{zx}^2) \right]^{1/2} \quad (2)$$

$\sigma_x$ ,  $\sigma_y$  and  $\sigma_z$  are principal normal stresses,  $I_{xy}$ ,  $I_{yz}$  and  $I_{zx}$  are principal shear stresses. The equations, which have been used for stress calculation during simulation, are as follows:

$$\varepsilon = \frac{1}{2} \left[ (\nabla u)^T + \nabla u \right] \quad (3)$$

$$\rho C_p \frac{\partial T}{\partial t} + \nabla \cdot (-k \nabla T + \rho C_p T u) = Q \quad (4)$$

where  $\varepsilon$  is the strain,  $u$  is the displacement,  $T$  is the temperature,  $\rho$  is the density,  $k$  is the thermal conductivity,  $C_p$  is the specific heat at

**Table 1**  
Sample composition along with their densities and CTE [14].

Sample name	Composition (1:1)	Density (gm cc <sup>-1</sup> )	CTE (RT-softening) × 10 <sup>-6</sup> K <sup>-1</sup>
GG1	ML + CL	3.42	9.36
GG2	CL + SL	3.68	9.92
GG3	SL + BL	4.01	10.89
GG4	BL + ML	3.82	9.32
GG5	BL + CL	3.91	7.05
GG6	ML + SL	3.54	10.01
GG7	ML + CL + SL + BL	3.85	9.77

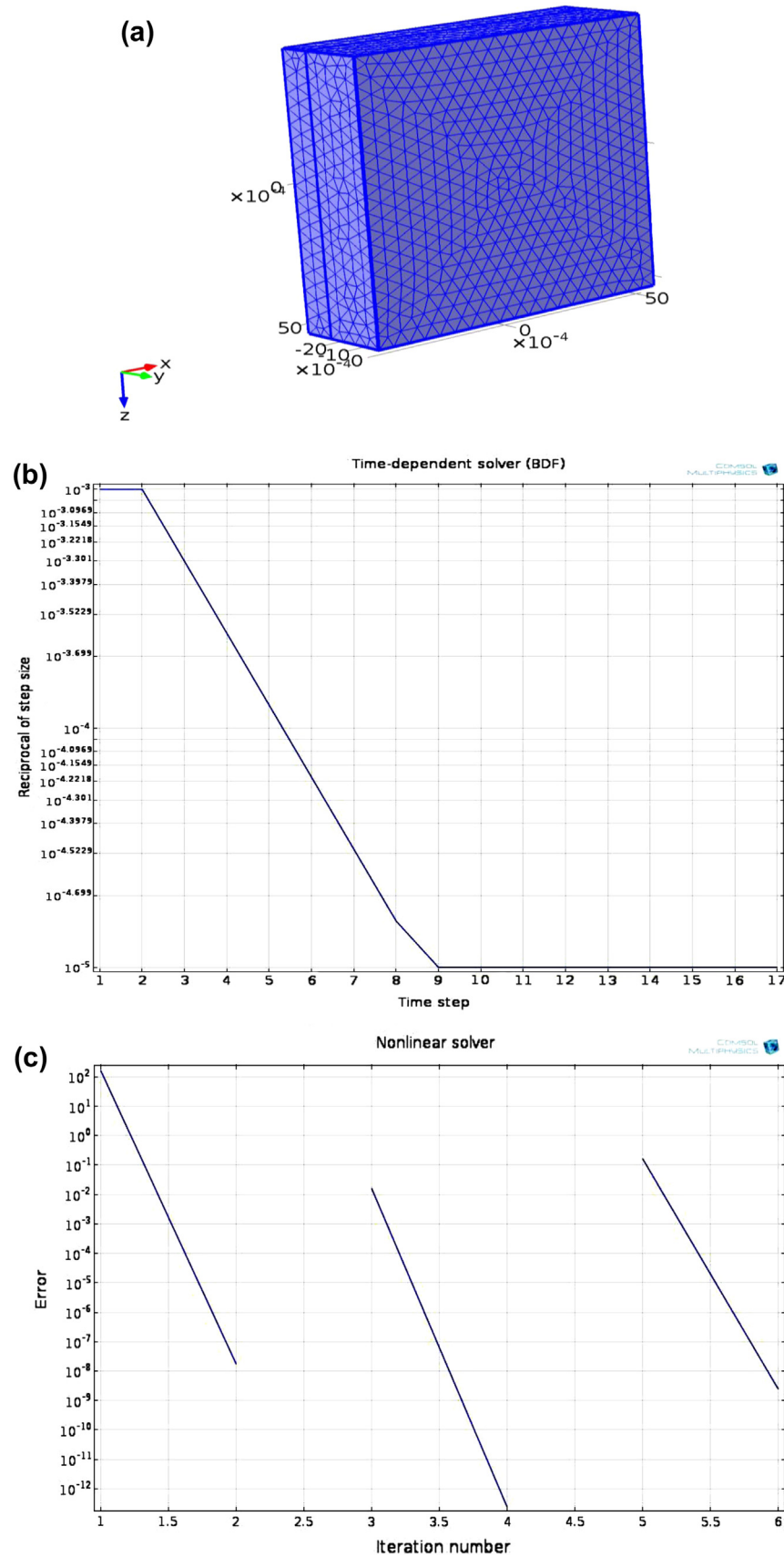


**Fig. 1.** (a) Fine mesh symmetry model of sample GG1/Crofer 22APU diffusion couple. (b) Convergent time dependent solver (BDF) of thermal stress calculations for sample GG1/Crofer 22APU diffusion couple. (c) Convergent non-linear solver of heat-flux calculations for sample GG1/Crofer 22APU diffusion couple.

constant temperature and  $Q$  is the heat source or sink. The thermal expansion can be determined by taking into consideration the attraction between ions as follows [24]:

$$F = 2Z/d^2 \quad (5)$$

where  $F$  is force of attraction,  $Z$  is charge of positive ions and  $d$  is the distance between positive and negative ions. If the interatomic potential well of an atom is parabolic, then the atomic displacement and driving force are linearly proportional to each other. In that case, the atoms undergo harmonic oscillation, without change in their position yielding no thermal expansion during heating process. Generally, the potential well is not parabolic as the Lennard-Jones potential and shows more resistance to compression than tension [24]. Hence, thermal vibrations tend to drive atoms apart causing thermal expansion. With increase of heat-treatment duration, the amplitude of thermal vibrations also gets enhanced. Furthermore, in the asymmetric potential well, the atoms spend more time at  $r > r_0$ , where  $r_0$  is the equilibrium distance at absolute zero. This may lead to a decrease in the attraction between ions and an increase in the bond length leading to expansion within the network. The main assumptions, which are implemented during finite element simulation using the COMSOL, are as follows:

- No exposure to external forces.
- Static linear elastic theory is valid.
- The temperature range is taken to be RT – 800 °C.
- The simulation has been done to obtain the thermal stress for 10,000 h of operation of SOFC.
- The geometry is two-layered structure exhibiting homogenous isotropic material properties.

Fig. 2(a)–(c) gives the stress distribution on the GG1 composite surface for its different thickness. Fig. 2(a) describes the stress for

composite thickness ( $t$ ) of 0.25 mm and the stress varies between  $2.64\text{E}-5$  and  $5.58\text{E}-3 \text{ N m}^{-2}$ . For  $t = 0.5 \text{ mm}$  (Fig. 2(b)), the stress varies between  $1.87\text{E}-6$  and  $4.55\text{E}-3 \text{ N m}^{-2}$  whereas the stress is between  $2.27\text{E}-6$  and  $2.74\text{E}-3 \text{ N m}^{-2}$  for  $t = 1.5 \text{ mm}$  (Fig. 2(c)). Crofer 22APU is stiffer than the glass composite and almost stress free. The stiffness of the material depends upon its thickness and elastic moduli [22]. The elastic moduli of the interconnect is 200 GPa and for all the composites it is between 120 and 140 GPa. Hence, a considerable amount of stress could be seen on the seal for different thickness corresponding to difference in CTE. The CTE for GG1 is  $9.36\text{E}-6 \text{ K}^{-1}$  and Crofer 22APU is  $11.3\text{E}-6 \text{ K}^{-1}$ , hence the difference in CTE ( $\Delta\alpha$ ) for the GG1 and Crofer 22APU is  $1.94\text{E}-6 \text{ K}^{-1}$ . For  $t = 0.25 \text{ mm}$ , the high stress region is on the surface of glass composite, whereas for  $t = 0.5$  and  $1.5 \text{ mm}$ , these regions are on the edge. But the overall distribution indicates that, the stress for most of the region is between  $1\text{E}-3$  and  $2\text{E}-3$ ,  $5\text{E}-4$  and  $2\text{E}-3 \text{ N m}^{-2}$  and  $5\text{E}-4$  and  $1\text{E}-3$  corresponding to  $t = 0.25$ ,  $0.5$  and  $1.5$  respectively. Hence the stress for  $t = 0.25 \text{ mm}$  is ten times more than the stress for  $t = 0.5$  and  $1.5 \text{ mm}$ . In contrast to this, the sample GG2/Crofer 22APU (Fig. 3(a)–(c)) diffusion couple gives lower stress values contributed by  $\Delta\alpha$  of  $1.38\text{E}-6 \text{ K}^{-1}$ . For  $t = 0.25 \text{ mm}$ , the stress varies between  $1.12\text{E}-5$  and  $3.28\text{E}-3 \text{ N m}^{-2}$  as is clear from Fig. 3(a). The stress for  $t = 0.5 \text{ mm}$  is between  $2.47\text{E}-6$  and  $2.8\text{E}-3 \text{ N m}^{-2}$  (Fig. 3(b)) and for  $t = 1.5 \text{ mm}$ , it lies within  $1.05\text{E}-6$  to  $2.10\text{E}-3 \text{ N m}^{-2}$  (Fig. 3(c)). For the GG2 composite, the high stress regions are on the edges as well as within the surface also for all thickness.

From Fig. 4(a)–(c), it is clear that the stress is small for the GG3/Crofer 22APU diffusion couple as compared to the GG1/Crofer 22APU and the GG2/Crofer 22APU couple. It is attributed to the small difference in the CTE for the glass composite GG3 and the Crofer 22APU i.e.  $0.41\text{E}-6 \text{ K}^{-1}$ . The major stress regions get concentrated on the edges as the thickness increases from  $0.25$  to  $1.5 \text{ mm}$ , though the stress decreases with the thickness. The stress decreases from

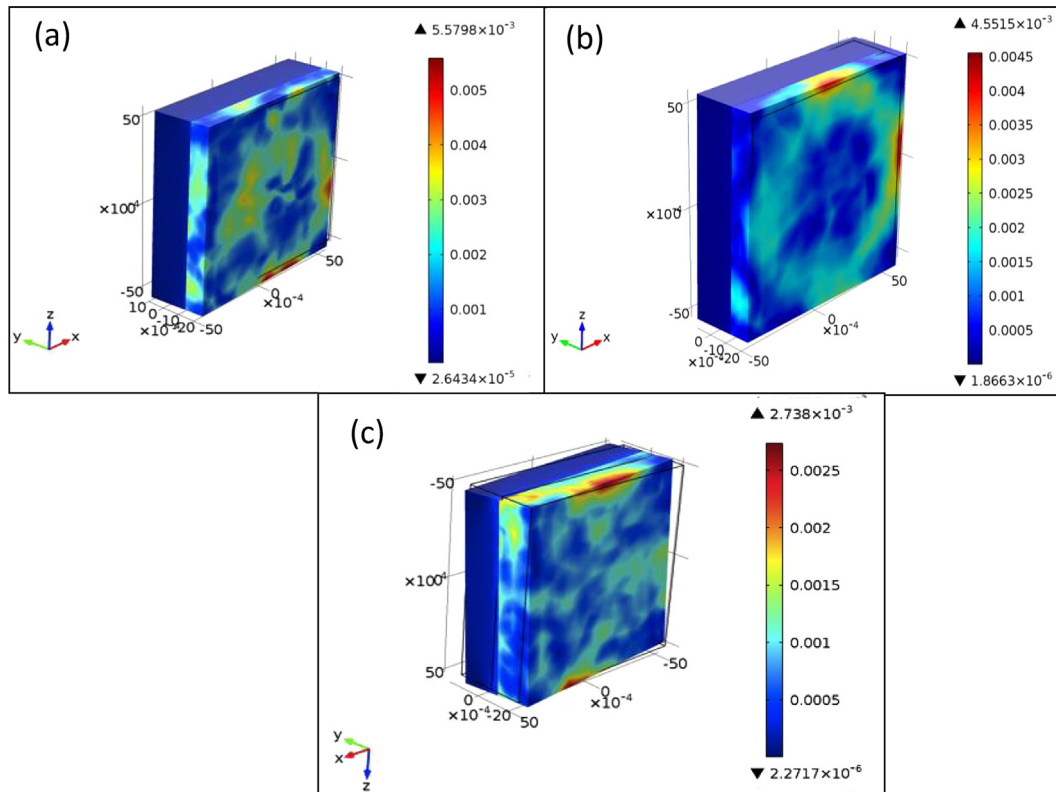
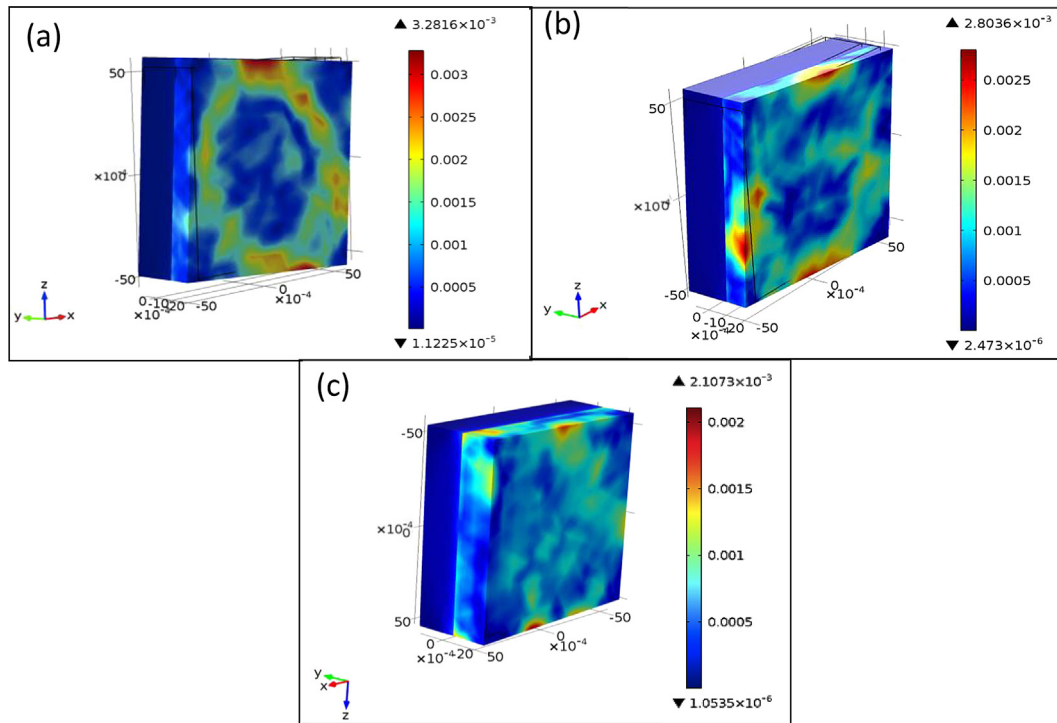
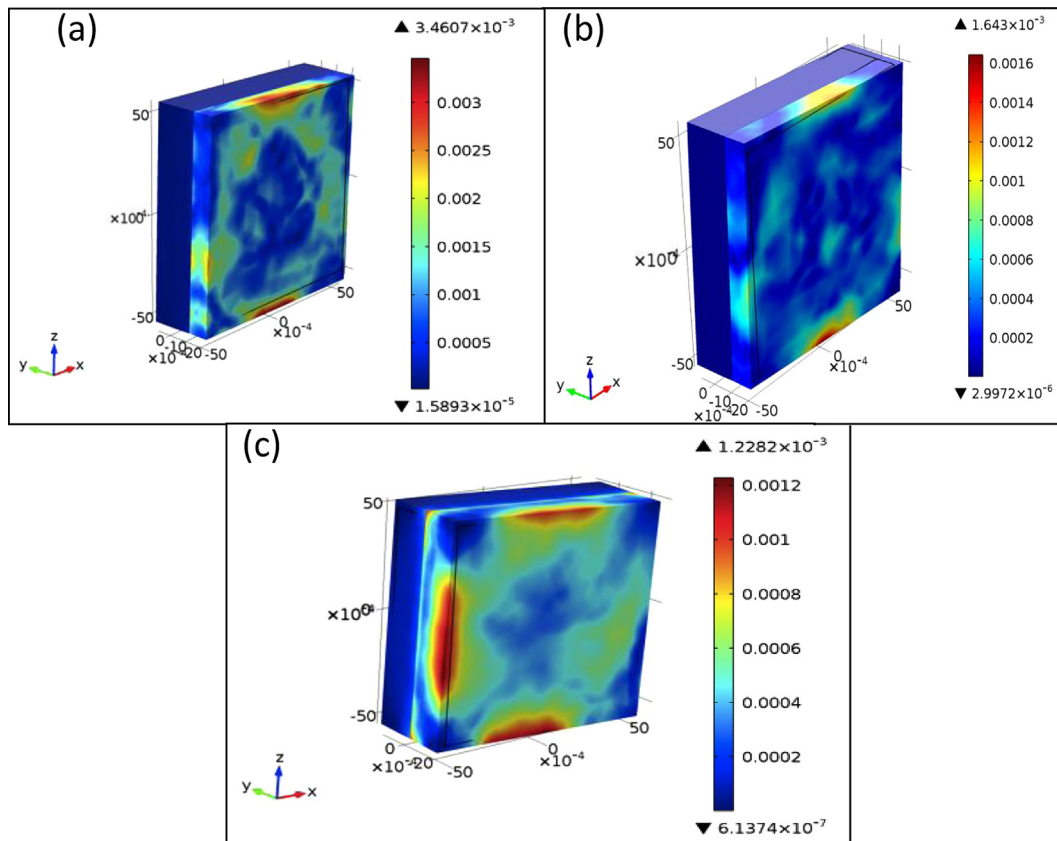


Fig. 2. The stress contours and their magnitude for the GG1/Crofer 22APU diffusion couple for thickness (a)  $t = 0.25$ , (b)  $t = 0.5$  and (c)  $t = 1.5 \text{ mm}$  (simulated upto 10,000 h, step size 1).



**Fig. 3.** The stress contours and their magnitude for the GG2/Crofer 22APU diffusion couple for thickness (a)  $t = 0.25$ , (b)  $t = 0.5$  and (c)  $t = 1.5$  mm (simulated upto 10,000 h, step size 1).



**Fig. 4.** The stress contours and their magnitude for the GG3/Crofer 22APU diffusion couple for thickness (a)  $t = 0.25$ , (b)  $t = 0.5$  and (c)  $t = 1.5$  mm (simulated upto 10,000 h, step size 1).



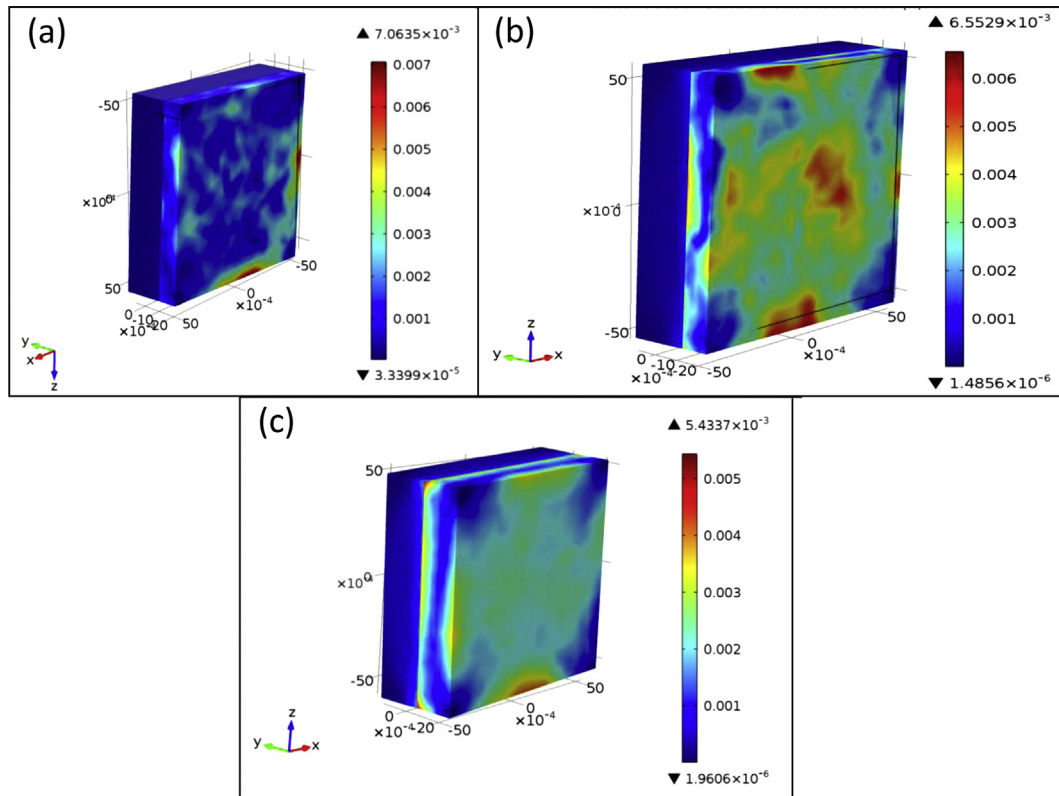


Fig. 5. The stress contours and their magnitude for the GG4/Crofer 22APU diffusion couple for thickness (a)  $t = 0.25$ , (b)  $t = 0.5$  and (c)  $t = 1.5$  mm (simulated upto 10,000 h, step size 1).

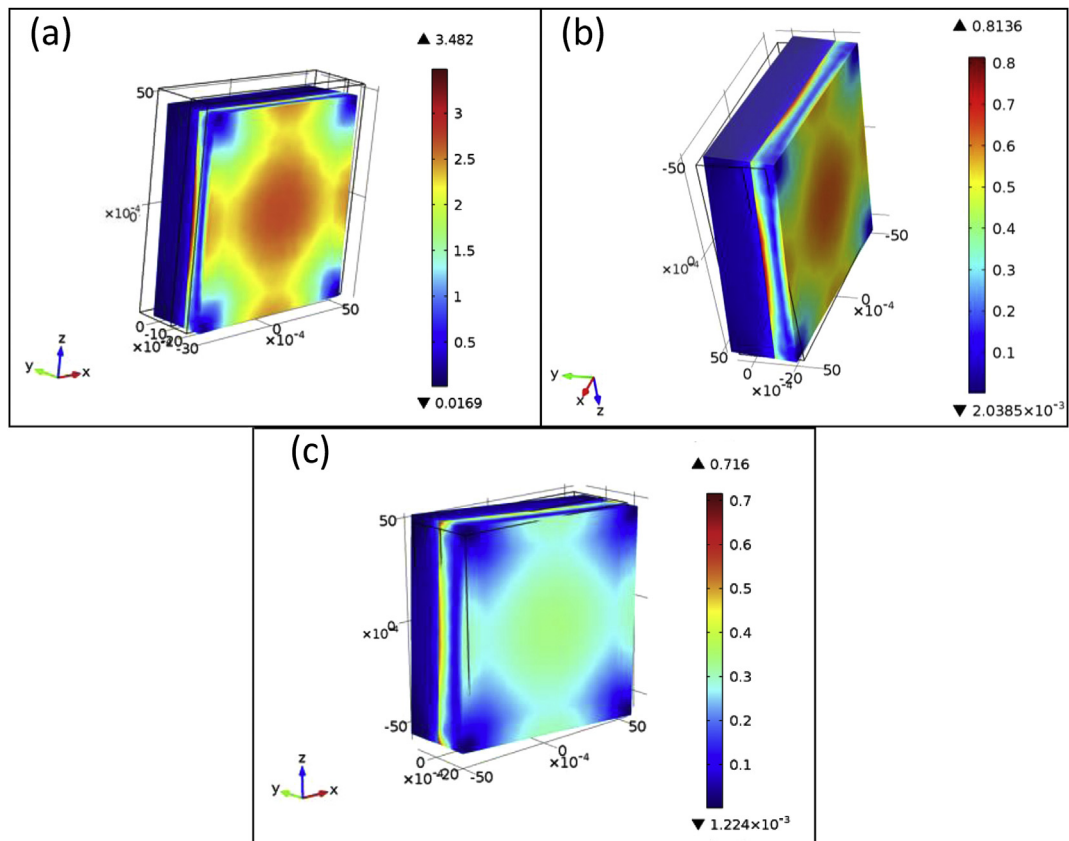


Fig. 6. The stress contours and their magnitude for the GG5/Crofer 22APU diffusion couple for thickness (a)  $t = 0.25$ , (b)  $t = 0.5$ , and (c)  $t = 1.5$  mm (simulated upto 10,000 h, step size 1).

$3.46\text{E}-3$  to  $1.22\text{E}-3$  with increase of thickness from 0.25 to 1.5 mm. Very small regions of high stress could be seen on the surface. The interface is mostly under the influence of normal stress rather than shear stress [18]. Composite GG3 is made up of  $\text{Sr}^{2+}$  and  $\text{Ba}^{2+}$  ions. From X-ray diffraction analysis of GG4 composite after a heat-treatment of 1000 h [14], it is apparent that barium silicate phase has been formed. These phases are high CTE phases and hence help in reducing the thermal stress around the interface or corners.

For the GG4/Crofer 22APU (Fig. 5(a)–(c)), the stress is more on the edge for  $t = 0.25$  and varies within  $3.34\text{E}-5$  to  $7.06\text{E}-3 \text{ N m}^{-2}$ . For  $t = 0.5$  mm, the high stress regions are more on surface than the edges as can be seen from Fig. 5(a). The stress for  $t = 0.5$  mm (Fig. 5(b)) varies between  $1.49\text{E}-6$  and  $6.55\text{E}-3 \text{ N m}^{-2}$ . There is sharp decrease observed in the maximum stress for  $t = 1.5$  mm i.e. the maximum stress is  $1.22\text{E}-3 \text{ N m}^{-2}$  (Fig. 5(c)). This clearly indicates the dependence of seal thickness on thermal stress.  $\Delta\alpha$  is observed to be  $1.98 \text{ K}^{-1}$  which is the second highest after the GG5 sample.

The GG5/Crofer 22APU diffusion couple (Fig. 6(a)–(c)) exhibits maximum stress due to the highest mismatch of CTE with the interconnect among all other samples.  $\Delta\alpha$  for GG5 sample is  $4.25 \text{ K}^{-1}$ , which is totally outside, the acceptable limit for SOFC functioning. High stress of  $3.48 \text{ N m}^{-2}$  is observed for  $t = 0.25$  mm (Fig. 6(a)). For  $t = 0.5$  mm, the stress varies between  $2.04\text{E}-3$  and  $0.81 \text{ N m}^{-2}$  as can be seen from Fig. 6(b). With the increase in seal thickness to 1.5 mm (Fig. 6(c)), the maximum stress becomes 0.716. During the experimental studies, the seal thickness was kept to be 0.5 mm [14]. Some pores were observed in the GG4 composite. As indicated by simulation results, delamination or pore formation could be observed after prolonged heat-treatment duration. Interestingly, the simulation results are in complete agreement with the experimental results elucidated in our previous studies [14]. It is

reported by our group that no adhesion is obtained between the GG5 composite and Crofer 22APU metallic interconnect. Subsequently, the couple was delaminated after prolonged heat-treatment of 1000 h. Moreover, a low CTE calcium silicate phase is formed for the GG5 composite after treatment of 1000 h as is evident from its XRD studies [14]. The formation of calcium silicate could have lead to thermal mismatch with the Crofer 22APU interconnect. It is apparent from Fig. 6(a)–(c) that high stress regions are observed at the interface. The center of surface of the GG5 composite is under very high stress. For most of the GG5 surface, the stress varies between 0.4 and  $0.8 \text{ N m}^{-2}$  at  $t = 0.5$ , which is indeed high as compared to other glass composites. This could lead to delamination as well as cracks within the composite which could provide an easy pathway for leakage.

From Fig. 7(a)–(c), it is quite clear that the stress is distributed more on the surface rather than the edges or the corners for GG6/Crofer 22APU diffusion couple. Corresponding to a thermal mismatch of  $1.29 \text{ K}^{-1}$ , the maximum stress region lies between  $1.5\text{E}-5$  and  $3.9\text{E}-3$ ,  $3.16\text{E}-6$  and  $2.07\text{E}-3$  and  $1.95\text{E}-6$  and  $1.79\text{E}-3 \text{ N m}^{-2}$  for  $t = 0.25$ , 0.5 and 1.5 mm respectively. For most of GG6 surface with  $t = 0.5$  mm, the stress variation is between  $5\text{E}-4$  and  $1.5\text{E}-3 \text{ N m}^{-2}$ . Unlike the sample GG6, sample GG7 has more stress on the edges than on its surface due to the thermal mismatch of  $1.53 \text{ K}^{-1}$  as revealed by Fig. 8(a)–(c). The maximum stress for the GG7 composite varies as  $4.06\text{E}-3$ ,  $2.89\text{E}-3$  and  $2.05\text{E}-3 \text{ N m}^{-2}$  for  $t = 0.25$ , 0.5 and 1.5 mm respectively. The simulation results indicate that stress follows the trend  $\text{GG5} > \text{GG4} > \text{GG1} > \text{GG7} > \text{GG2} > \text{GG6} > \text{GG3}$  for  $t = 0.5$  mm. This is in exact correlation with the results obtained for the thermal expansion studies. Stresses generated in the component can deform the seal elastically or plastically. A number of parameters can be tailored to reduce the stress among the components, which

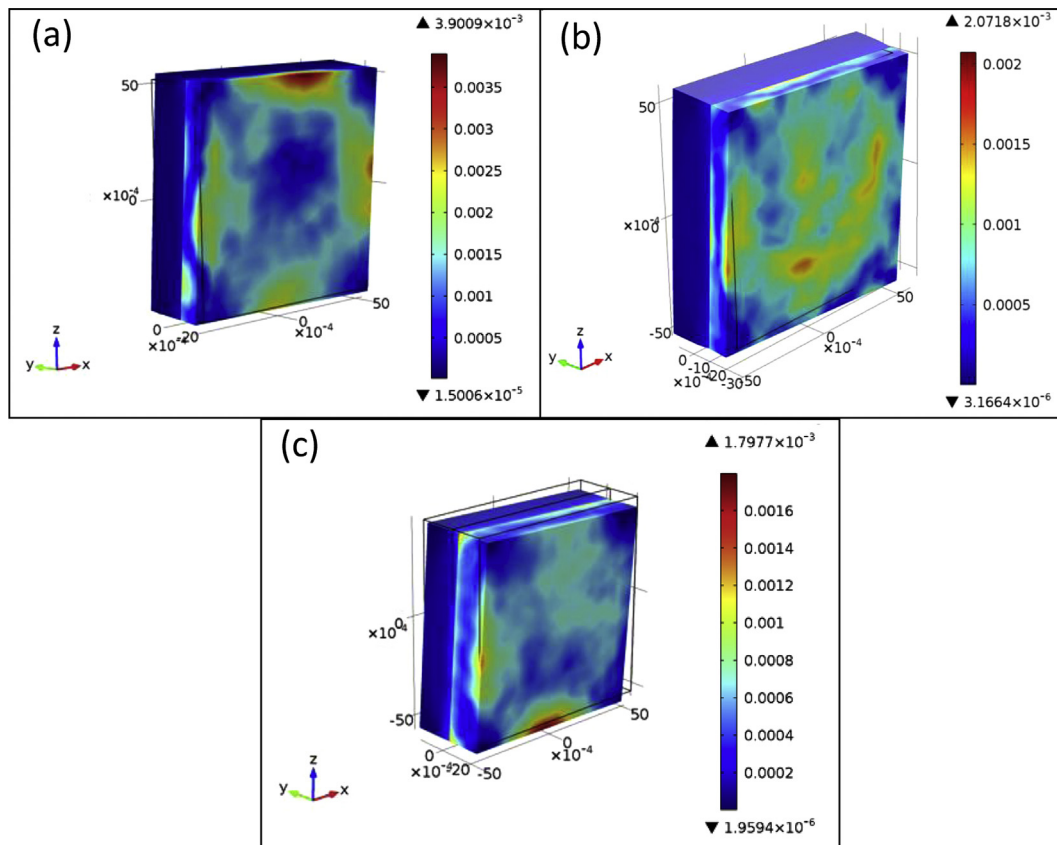
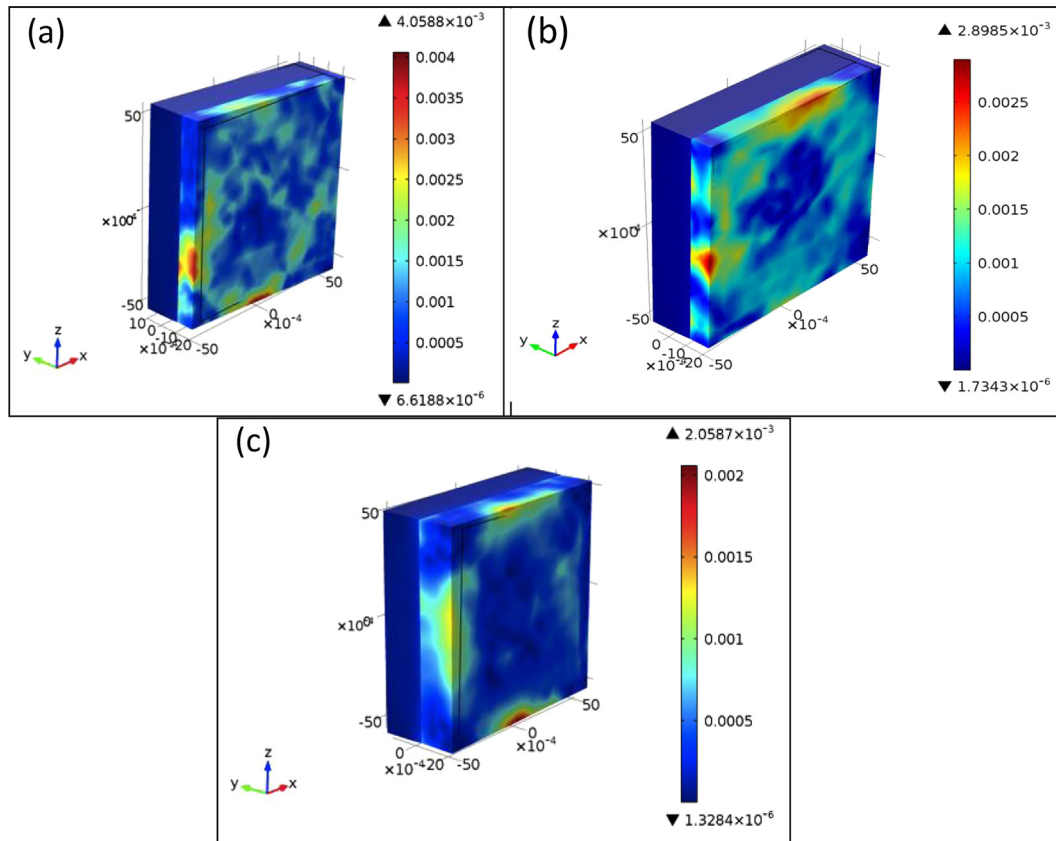


Fig. 7. The stress contours and their magnitude for the GG6/Crofer 22APU diffusion couple for thickness (a)  $t = 0.25$  (b)  $t = 0.5$  and (c)  $t = 1.5$  mm (simulated upto 10,000 h, step size 1).



**Fig. 8.** The stress contours and their magnitude for the GG7/Crofer 22APU diffusion couple for thickness (a)  $t = 0.25$ , (b)  $t = 0.5$  and (c)  $t = 1.5$  mm (simulated upto 10,000 h, step size 1).

include thickness, CTE, composition and elastic modulus. In the present investigation, the seal thickness was changed from 0.25 to 1.5 mm. It has been observed that when the thickness is increased then the deformation due to stress is small which is in accordance with the results obtained by Weil [25]. Weil [25] has shown that increasing the seal thickness reduces the thermal stress. All the composites except the GG7 composite exhibit 10 times more thermal stress when  $t = 0.25$  mm in comparison to  $t = 0.5$  and 1.5 mm. The simulated heat-flux for the sample GG7/Crofer 22APU is shown in Fig. 9. The heat-flux was simulated in order to investigate if there is

any temperature gradient about the interface, or within the layers. Isothermal contours are obtained for the sample GG7 upto 1000 °C for a 10,000 h heat-treatment.

#### 4. Conclusions

COMSOL analysis was performed to determine the stress within the composite seal/Crofer 22APU after prolonged duration of heat-treatment for 10,000 h. It has been observed that when the composite seal thickness is increased from  $t = 0.25$  to 1.5 mm, then the deformation due to stress is small. Maximum stress was observed within the GG5 composite seal attributed to its maximum CTE mismatch. In contrast to this, the minimum stress is observed for the GG3 at  $t = 0.5$  mm composite owing to small  $\Delta\alpha = 0.41$  which is within the acceptable limit of the CTE mismatch. Interestingly, for all the diffusion couples, no high stress regions could be obtained at the corners. Based on these simulation studies, it could be concluded that except the GG5 and GG4 composite samples, other samples exhibit good performance and less stresses. This further indicates the potential for hermeticity for these seals to achieve long-term performance goals for SOFC applications.

#### Acknowledgment

Authors are thankful to CIES, Washington D.C. for the financial assistance. One of the authors (GK) is thankful to Dr. Vishal Kumar, Yujie-Cheng and Cary Hill, Virginia Tech for their consistent support and guidance.

#### References

- [1] B.C.H. Steele, A. Heinzel, *Nature* 414 (2001) 345–352.
- [2] N.Q. Minh, *Solid State Ionics* 174 (2004) 271–277.

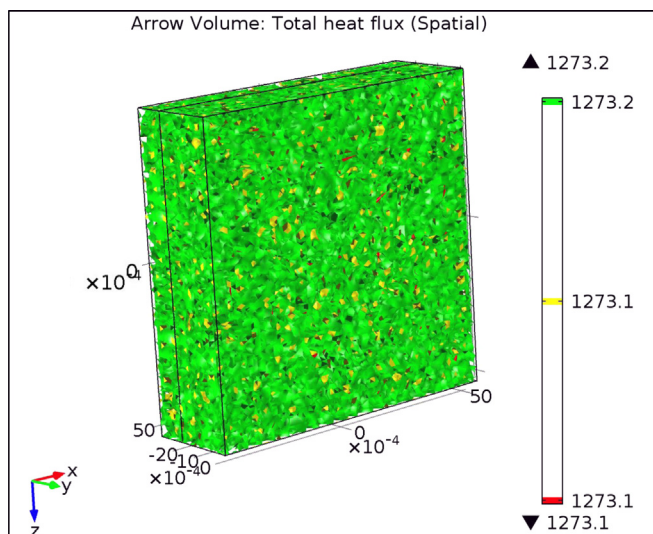


**Fig. 9.** Isothermal contours of heat-flux for GG7/Crofer 22APU.



- [3] S.C. Singhal, K. Kendall, High Temperature Solid-Oxide Fuel Cells: Fundamentals, Elsevier, New York, 2000, p. 14.
- [4] J.W. Donald, P.M. Mallinson, B.L. Metcalfe, L.A. Gerrard, J.A. Fernie, J. Mater. Sci. 46 (2011) 1975–2000.
- [5] S.M. Haile, Acta Mater. 51 (2003) 5981–6000.
- [6] K.S. Weil, C.A. Coyle, J.S. Hardy, J.Y. Kim, G.G. Xia, Fuel Cells Bull. (2004) 12–16.
- [7] A. Goel, M.J. Pascaul, J.M.F. Ferreira, Int. J. Hydro. Energy 35 (2010) 6911–6923.
- [8] M.K. Mahapatra, K. Lu, Mater. Sci. Eng. R 67 (2010) 65–85.
- [9] J.W. Fergus, J. Power Sources 147 (2005) 46–57.
- [10] G. Kaur, O.P. Pandey, K. Singh, Int. J. Hydrogen Energy 37 (2012) 3883–3889.
- [11] G. Kaur, O.P. Pandey, K. Singh, Int. J. Hydrogen Energy 37 (2012) 6862–6874.
- [12] G. Kaur, O.P. Pandey, K. Singh, Fuel Cells 12 (2012) 739–748.
- [13] F. Smeacetto, M. Salvo, M. Ferraris, V. Casalegno, P. Asinari, J. Eur. Ceram. Soc. 28 (2008) 611–616.
- [14] G. Kaur, O.P. Pandey, K. Singh, D. Homa, B. Scott, G. Pickrell, J. Power Sources 240 (2013) 458–470.
- [15] J.E. Shelby, Introduction to Glass Science and Technology, second ed., The Royal Society of Chemistry, Cambridge, 2005.
- [16] H.T. Chang, C.K. Lin, C.K. Liu, S.H. Wu, J. Power Sources 196 (2011) 3583–3591.
- [17] R. Hill, D. Gilbert, J. Am. Ceram. Soc. 76 (1993) 417–425.
- [18] W.N. Liu, X. Sun, M.A. Khaleel, J. Power Sources 196 (2011) 1750–1761.
- [19] A. Muller, J. Hohe, S. Goswami, W. Becker, in: L. Librescu, P. Marzocca (Eds.), Proceedings of Thermal Stresses '03 – The Fifth International Congress on Thermal Stresses and Related Topics (2003), Blacksburg, Virginia, USA, p. MA-7-4-1.
- [20] K.S. Weil, J. Mater. 58 (2006) 37–44.
- [21] J. Malzbender, R.W. Steinbrech, J. Power Sources 173 (2007) 60–67.
- [22] T. Zhang, Q. Zhu, Z. Xie, J. Power Sources 188 (2009) 177–183.
- [23] J.C. Jong, Teaching Von Mises Stress: From Principal Axes Tonon-Principal Axes, Springer, 2009. Am. Soc. Eng. Edu.
- [24] P. Jinhua, S. Kening, Z. Naiqing, C. Xinbing, J. Rare Earths 25 (2007) 434–438.
- [25] K.S. Weil, B.J. Koeppe, Int. J. Hydrogen Energy 33 (2008) 3976–3990.